High-precision freeform optics …the shape of some important things to come

G.W. Forbes
QED Technologies Inc., 1040 University Ave., Rochester, NY 14607, USA
forbes@qedmrf.com

Abstract: An array of applications drives the development of freeform optics. Tailored orthogonal polynomials are becoming more widely used for characterizing the nominal shapes of rotationally symmetric aspheres and their generalization to freeforms is discussed here.

Keywords: freeform optics, optical design, optical fabrication, optical metrology

1. Introduction

Tailored orthogonal polynomials have been introduced for characterizing the nominal shape of rotationally symmetric aspheres[1]. These ideas have recently been generalized for application to a wide class of freeform optics[2]. This approach benefits from effective, elegant numerical methods based on recurrence relations. The associated algorithms were shown to allow the surface shape to be computed efficiently along with derivatives of any order. By construction, the spectrum of coefficients that underlies this characterization offers an interpretation of shape at a glance and it facilitates simple estimates of manufacturability. Because the recurrence relations enable these methods to be used to arbitrarily high orders, the metrology data for real parts —regardless of whether they're nominally freeform— can also be characterized by using these intuitive spectra.

As suggested in Fig.1, there are two aspects to characterizing a freeform optic: (i) the shape of its face and (ii) the perimeter's shape. It is typically only the face that must be specified to sub-wavelength precision and it therefore stands as the focus of this discussion. Orthogonalization is necessarily performed over a specific domain and, rather than let the perimeter complicate things unnecessarily, the domain adopted here is simply a circular region that encloses the part's edge. This notionally circular region is created, as depicted in Fig.2, by enclosing the surface segment of interest within a cylinder. This cylinder will often be chosen to be nominally normal to the surface segment, as shown. It is then helpful to introduce a coordinate system aligned to the cylinder with its origin at the intersection of the cylinder's axis and the surface itself. These steps set the scene for the basis discussed here.

2. Orthogonalization

Surface sag is commonly expressed as a conic base with an additive deviation in the form of a polynomial. When that polynomial basis is orthogonalized, the associated coefficients become a spectrum of the surface's frequency content that can be interpreted readily upon inspection. Because the rate of change of the departure along the normal from a best-fit sphere is oftentimes a primary consideration, it is helpful to characterize surfaces by explicit reference to a best-fit sphere. Additionally, the orthogonalization can be tailored to this context further by adopting the mean square gradient of the normal departure from best-fit sphere as the underlying metric.

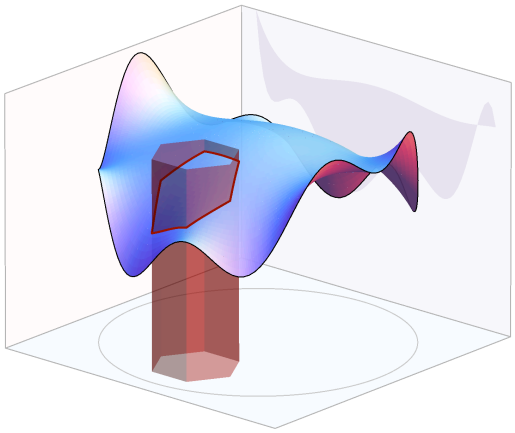

Fig.1. The segment of interest of this freeform surface is the intersection of a hexagonal column with the parent surface. The red curve is the part's perimeter while the section of the parent that lies inside the column is the part's face.

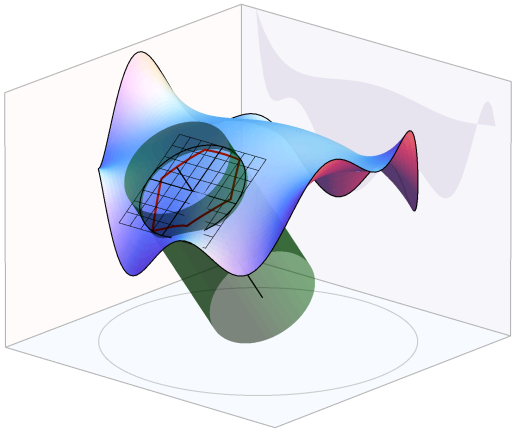

Fig.2. The freeform segment of Fig.1 can be characterized by first introducing an enclosing cylinder with an associated coordinate system.

Accordingly, the surface sag is expressed here in terms of cylindrical polar coordinates as

$$z(r,\theta) = \frac{c\,r^2}{1+\sqrt{1-c^2r^2}} + \frac{1}{\sqrt{1-c^2r^2}}\,\delta(u,\theta), \qquad (1)$$

where c is the curvature of the best-fit sphere, u is the normalized transverse coordinate (just r divided by the radius of the enclosing cylinder) and $\delta(u,\theta)$ is expressed in a Zernike-like form:

$$\delta(u,\theta) = u^2(1-u^2)\sum_{n=0}^{N} a_n^0 Q_n^0(u^2) + \sum_{m=1}^{M} u^m \sum_{n=0}^{N} [a_n^m \cos(m\theta) + b_n^m \sin(m\theta)] Q_n^m(u^2). \quad (2)$$

Here, $Q_n^m(v)$ is a polynomial of order n in v, and although they now carry a superscripted zero, the terms in the sum on the first line involve precisely the entities that are the subject of Ref.1. The second line holds new polynomials that, as defined in Ref.3, are orthonormal with respect to the weighted average of the inner product of their gradients. If angle brackets are used to denote this weighted average, it follows that the mean square gradient is given by just a sum of squares of the coefficients:

$$\left\langle |\nabla \delta(u,\theta)|^2 \right\rangle = \left\langle \left(\frac{\partial \delta}{\partial u}\right)^2 + \frac{1}{u^2}\left(\frac{\partial \delta}{\partial \theta}\right)^2 \right\rangle = \sum_{m,n} [(a_n^m)^2 + (b_n^m)^2]. \quad (3)$$

This powerful result underpins many of the strengths of Eqs.(1) and (2), and these three equations completely determine the form of $Q_n^m(v)$. It is interesting to note that a related set of polynomials was introduced by Zhao and Burge for entirely different purposes[3].

3. Demonstration

As a simplistic demonstration of this process that is also valuable for code verification, it is helpful to characterize an off-axis section of a paraboloid in the manner described above. In such a case with axial curvature of 1/20mm and an off-axis displacement of 20mm, these fit coefficients were given in Ref.2 when the enclosing cylinder is taken to be 20mm in diameter.

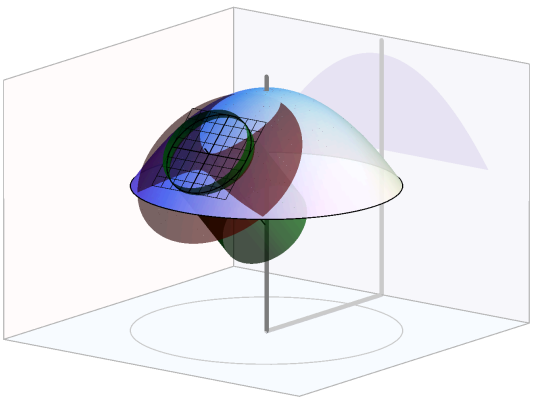

Fig.3. An off-axis section of a paraboloid can be fitted as a simple demonstration. The best-fit sphere that was adopted here is shown in red.

By including the 23 terms up to eighth order, sub-nm fit accuracy is achieved for this case. (Of course, the plane of symmetry means that $b_n^m \equiv 0$, so they are not included.) The tilt of the cylinder drawn in Fig.3 is chosen so that $a_0^1 = 0$ and, as a result, the difference in sag plotted in Fig.4 has a non-zero tangent at the centre. The associated fit coefficients reveal at a glance that the departure is dominated by the astigmatism term (at about 500μm). That is, the challenge of fabricating such an asphere can be appreciated by glancing at the coefficient values; there is no longer any need to evaluate sag samples or do any best fitting. This is just one of the advantages of this tailored characterization of shape. Others are to be covered in the talk.

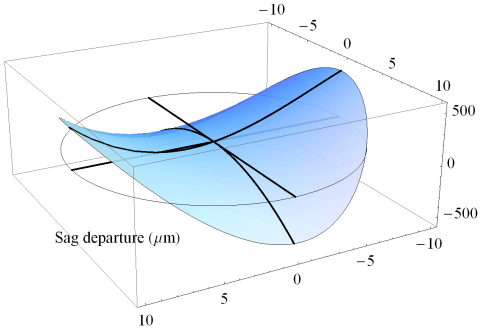

Fig.4. The departure between the paraboloid of Fig.3 and its best-fit sphere. The cylinder was oriented so that the mean tilt in the normal departure is zero over this circular domain.

4. Concluding remarks

While no single convention for characterizing shape can possibly meet all the requirements of the wide range of applications of freeform optics, the one discussed here meets many of those needs. The fact that Qbfs of Ref.1 is contained as a special case gives this framework a distinct advantage. The associated coefficients have been shown to be effective degrees of freedom for design. More generally, they provide "neat numbers" for communicating shape in an efficient way that admits robust computation to any level of complexity. Further, measures of manufacturability can often be expressed in terms of the differences between the local principal curvatures on the surface, and it is significant that the mean square value of that difference can be approximated readily as a quadratic in the fit coefficients of Eq.(2). It is also worth noting that metrology data of real parts can be reduced to spectra of the sort described here, thereby offering a possible quantification of mid-spatial frequency structure.

With the growth of applications of freeform optics in systems like head-up and head-mounted displays as well as in various projection systems —such as EUV lithography— there is little doubt that freeforms will play a vital role in important developments that are currently underway. An effective general-purpose characterization of shape like that discussed here can therefore facilitate key steps in this production chain.

5. References

1) G.W. Forbes: Opt. Exp. **18**(19), 19700–19712 (2010)
2) G.W. Forbes: submitted to Opt. Exp. in Nov 2011
3) C. Zhao and J.H. Burge: Opt. Exp. **15**(26), 18014-18024 (2007)